Indian Geotechnical Journal, 36 (3), 2006, 249-271

Analysis and Settlement of a Non-Homogeneous Granular Pile

M. R. Madhav*, J. K. Sharma and S. Chandra*****

Introduction

The need for ground improvement in civil engineering projects has become imperative due to non-availability of good construction sites and the presence of extensive deposits of loose or soft soil. In recent years, the use of sand compaction piles (SCP) /granular piles (GP) has been recognised as an efficient and cost-effective method of reinforcing soft cohesive soils, silts and loose granular deposits to sustain structural foundations for light to moderately loaded buildings. The method involves the replacement of 10-35% of the soft or loose soil with columns of coarse granular material such as crushed stone or coarse dense sand (Shamoto et al., 1997; Hu et al., 1997). The inclusion of stiffer, less compressible granular material increases the load carrying capacity and reduces the settlement of foundations built on the reinforced ground to an acceptable level. The columns of granular material also help to speed up consolidation effects in the soft ground. Granular piles/gravel drains in potentially liquefiable cohesionless deposits dissipate rapidly the pore pressures generated due to repeated earthquake loading (Seed and Booker, 1977; Baez and Martin, 1992).

A number of analyses have been developed for estimating the settlement of sand compaction pile/granular pile reinforced ground based on the unit-cell concept and on empirical estimates. Using the unit cell approach, parametric solutions have been obtained employing the analytical (Balaam and Booker, 1981; Van Impe and Madhav, 1992; Alamgir et al., 1996; Poorooshasb and Meyerhoff, 1997) and the finite element (Schweiger and Pandey, 1986; Canneta and Nova, 1989) methods. Empirical estimates of the improvements effects have been developed based on load tests or SPT values of improved ground (Nakayama et al., 1973; Nayak, 1983; Bhandari and Nayak, 1984; Solymar et al., 1986; Mizuno et al., 1987; Shamoto et al., 1997).

Mattes and Poulos (1969) and Poulos and Mattes (1969) based on continuum approach analysed single compressible floating and end bearing

---

* Emeritus Professor, Department of Civil Engineering, J.N.T.University, Hyderabad - 500 072, India. Email: madhav@iitk.ac.in

** Senior Lecturer, Department of Civil Engineering, Engineering College, Kota - 324 010, India

*** Professor, Department of Civil Engineering, Indian Institute of Technology Kanpur, Kanpur - 208 016, India

piles and presented parametric solutions in the form of design charts. Butterfield and Banerjee (1971) analysed a single compressible pile and pile groups using the boundary integral method and studied the effects of various deformation parameters related to the soil and the pile.

A number of solutions are available for estimating settlement of soft ground treated with granular piles having constant modulus of deformation i.e., homogeneous granular pile. The consideration of non-homogeneity of granular pile is more realistic and would reflect the interaction more accurately between the granular pile and the soil. Many factors related to non-homogeneity of granular pile in terms of its deformation modulus are conceivable and discussed below:

1. Installation of sand compaction pile/granular pile requires a proper insight into and understanding of the site conditions. Various techniques have been used the world over to install granular piles depending upon the proven applicability and availability of equipment in the locality. Vibro-floatation (Greenwood and Kirsch, 1983), rammed stone column (Datye and Nagaraju, 1975) and vibro-compozer (Aboshi et al., 1979) are some of the common techniques. Granular piles are constructed in stages with granular material placed in lifts in the hole and compacted. Though the energy input for compaction at each stage of construction of granular pile may be constant, increasing in-situ confining stresses of surrounding soil with depth may lead to different degrees of compaction and unit weights with depth leading to non-homogeneity of granular pile in terms of its deformation modulus.

2. Non-homogeneous granular pile material used at different stages of construction may be the other cause for non-homogeneity.

3. Much evidence is now available that freshly deposited or densified saturated granular material may exhibit substantial stiffening and strength increase with time up to several months (Mitchell and Solymar, 1984). The effects of this phenomenon may lead to non-homogeneity of granular pile.

4. From the field study of Baez and Martin (1995) on vibro-stone columns based on shear wave velocity test, the shear modulus of stone column material has been found to vary linearly with depth in the 'King Harbour tests'. The results indicate that shear modulus ratio, G_r, (the ratio of shear modulus of stone column to that of improved soil) varies with depth between 1 and 8 for well graded stone columns, whereas it varies between 1 and 6 for poorly graded stone columns. A "best fit" linear relationship is also shown in Fig. 1. It is also interesting to note that the "best fit line" for the poorly graded column material data has the same slope as that for the well graded data. These results have the relevance and represent the non-homogeneity of granular pile. Variations in these parameters may lead to non-homogeneity of granular pile in terms of its deformation modulus. The simplest way of approximating this non-homogeneity of granular pile is to consider its deformation modulus to increase linearly with depth from ground surface or top to its tip.

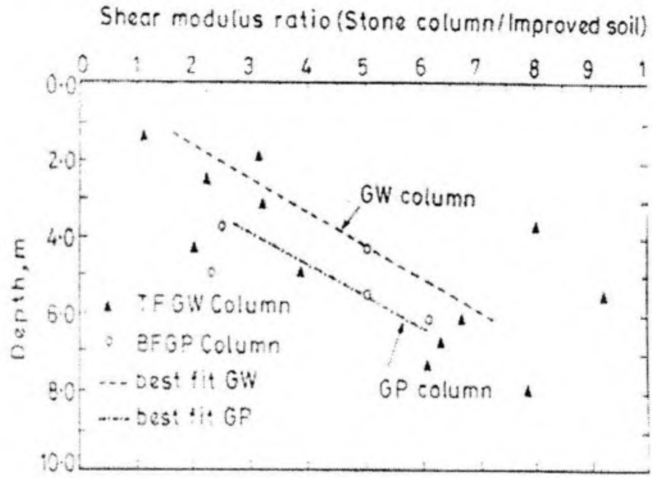

Fig. 1 Variation of Shear Modulus Ratio with Depth (Baez and Martin, 1995)

Problem Definition and Method of Analysis

Figures 2 (a) and (b) show respectively end bearing and floating granular piles of diameter, d, and length, L, acted upon by a load P. The granular pile is compressible and is characterised by the deformation modulus, E_{gp}, increasing linearly with depth. The deformation modulus $E_{gp}(z)$ at any depth, z, from the top of the granular pile is

$$E_{gp}(z) = E_{gp0}(1 + \eta \frac{z}{L}) \quad (1)$$

Where, E_{gp0} is the deformation modulus at the top and η -a non-homogeneity parameter which can be expressed as

$$\eta = \frac{E_{gpL} - E_{gp0}}{E_{gp0}} \quad (2)$$

where, E_{gpL} is the deformation modulus of the granular pile at the tip. The surrounding soil and the base are represented by their deformation moduli and Poisson's ratios as E_s and ν_s and E_b and ν_b respectively. The relative stiffness parameter is defined as the ratio of the deformation modulus of the granular pile at ground level to that of the soil i.e., K_{gp0} (= E_{gp0}/E_s). The relative stiffness of the bearing stratum is expressed as E_b/E_s.

The elastic continuum approach is employed to analyse the behaviour of a non-homogeneous granular pile in an ideal elastic soil mass. The basic assumptions in the analyses are:

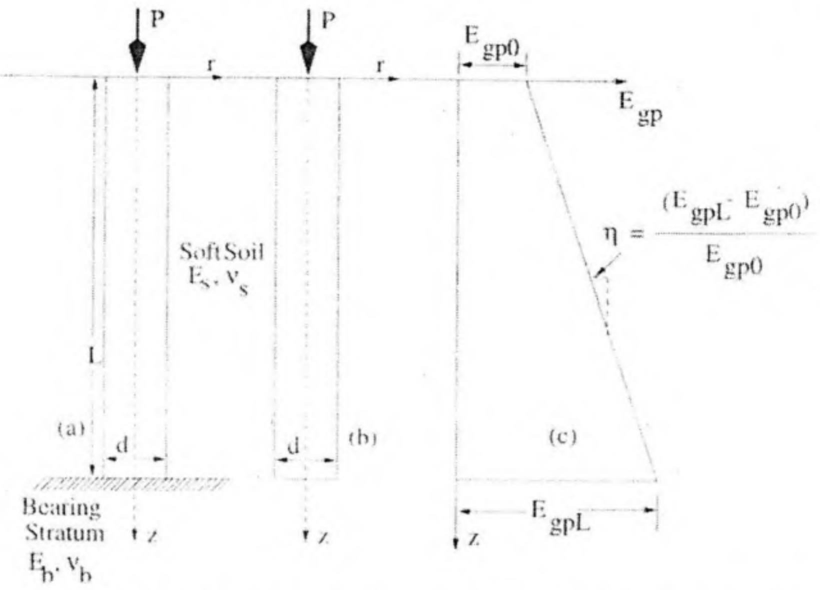

Fig. 2 Definition Sketch – Non-homogeneous Granular Pile, (a) End Bearing, (b) Floating, (c) Variation of Modulus of Deformation with Depth

1. The analysis presented is based on the linear stress-strain behaviour of granular pile material and surrounding soil.

2. The stone column base is assumed to be smooth and rigid across which the load is uniformly distributed.

3. The disturbance effects in the *in situ* soil due to the installation of granular piles are ignored and considered as homogeneous.

4. The settlement of granular pile depends on its deformation modulus and geometry besides the magnitude of load. Based on the various studies as discussed above, the consideration for the non-homogeneity of granular pile is appropriate and close to *in situ* behaviour. Non-homogeneity of granular pile is considered in terms of its deformation modulus with the linear variation.

The load on GP is shared by mobilisation of shear stresses on GP-soil interface and base pressure. The analysis is based on finding out the stress system, $\{\tau\}$, along the soil-granular pile interface and the base stress, p_b, which satisfy the compatibility of displacements along the interface for no slip or yield condition (Mattes and Poulos, 1969). The essential steps of the analysis are:

(1) Discretisation (Fig.3) for numerical integration of Mindlin's equation for the vertical displacement due to vertical stresses is used for calculating the soil displacements at the midpoint on the periphery of each element. To account the influence of the bearing stratum in case of end-bearing GP, the mirror-image technique is used.

(2) Elemental displacements of floating GP are computed based on the equilibrium relation for an infinitesimal element (Mattes and Poulos, 1969) with the consideration of non-homogeneity parameter, η of GP. In case of end bearing, the GP displacements are calculated with the consideration of finite compressibility of bearing stratum. Settlement of any element 'i' is estimated as the settlement of the element 'i+1' plus the settlement of the element due to axial stress acting on it.

(3) Through the compatibility of displacements of the granular pile and the soil, solution is obtained in terms of interface shear stresses and displacements.

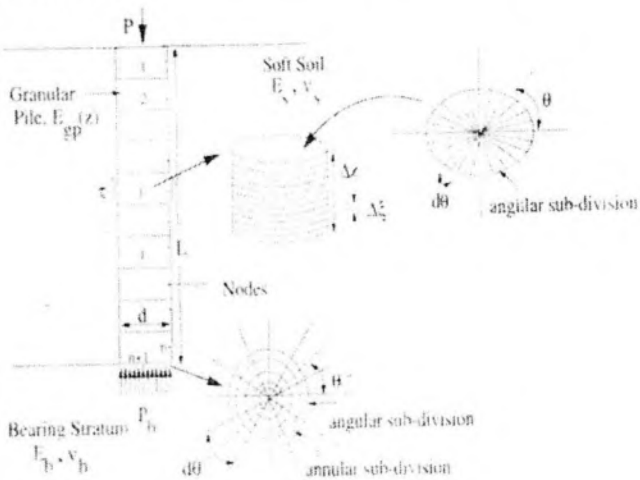

Fig. 3 Discretisation Scheme

Soil Displacements

The GP is discretised into n cylindrical elements acted upon by shear stresses (τ) and with the base having a uniform pressure (p_b). The discretisation used for the integration of Mindlin equation is shown in Fig. 3. The granular pile base is assumed to be smooth, across which the load is uniformly distributed. The soil displacements of the nodes on GP periphery and the centre of each element are evaluated based on the influence of the elemental shear stresses. Thus soil displacements equations for a floating granular pile are

$$\left\{\rho^s\right\} = \left\{\frac{S^s}{d}\right\} = \left[I_s\right]\left\{\frac{\tau}{E_s}\right\} \tag{3a}$$

and for a granular pile resting on a stiff bearing stratum (Poulos and Mattes, 1969)

$$\left\{\rho^s\right\} = \left\{\frac{S^s}{d}\right\} = \left[\left[I_s\right] - \kappa\left[I_{sim}\right]\right]\left\{\frac{\tau}{E_s}\right\} \tag{3b}$$

where $\{S^s\}$ and $\{\rho^s\}$ are soil displacement and normalised soil displacement vectors respectively. $\{\rho^s\}$ is size of (n+1) and 'n' for floating and end bearing GPs respectively. In case of floating granular pile, $\{\tau/E_s\}$ is a column vector of size (n+1) for the normalised shaft stresses and normal stress on the base while in case of end bearing GP it is column vector of size 'n' excluding the base pressure. To account for the influence of the bearing stratum, the mirror image approximation (Poulos and Mattes, 1969) is used. The influence of the mirror image elements is taken as, κ, times the influence of shear stresses on the real elements in the negative direction where, κ is a non-dimensional parameter that accounts for the compressibility of the base and lies between 0 and 1 for floating GP and GP resting on a rigid stratum respectively (Fig. 4). $[I_s]$ is a square matrix of soil displacement influence coefficients of size (n+1) and 'n' for floating and end bearing GP respectively. $[I_{sim}]$ is a square matrix of soil displacement influence coefficients due to image elements of size 'n'.

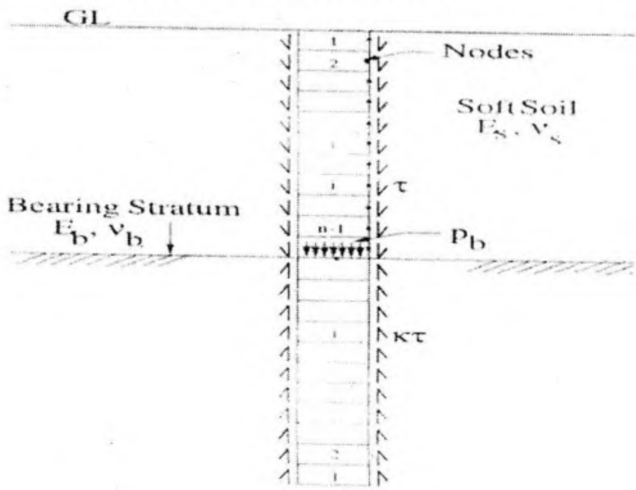

Fig. 4 Mirror-Image Technique for Granular Pile Resting on Bearing Stratum

Pile Displacements

GP displacements for floating and end bearing GP resting on relatively stiff bearing stratum are obtained as follows:

Floating Granular Pile: GP displacements are obtained based on the equilibrium relation for an infinitesimal element of GP (Mattes and Poulos, 1969) as

$$\frac{d\sigma_z}{dz} = -\frac{4\tau}{d} \tag{4}$$

where σ_z and τ are the axial and shear stresses at depth z. Considering the axial strain in the element, it is readily seen that

$$\varepsilon_z = -\frac{dS^p}{dz} = \frac{\sigma_z}{E_{gp}(z)} = \frac{\sigma_z}{E_{gp0}(1+\eta\frac{z}{L})} \tag{5}$$

where S^p is pile displacement and $E_{gp}(z)$ is the deformation modulus of granular pile at depth z. Differentiating Eqn. (5) with respect to z and substituting it in Eqn. (4), one gets

$$E_{gp0}\left[\frac{\eta}{L}\frac{dS^p}{dz} + (1+\frac{\eta z}{L})\frac{d^2S^p}{dz^2}\right] = \frac{4\tau}{d} \tag{6}$$

The following non-dimensional parameters are selected:

$$\rho^p = \frac{S^p}{d},\ K_{gp0} = \frac{E_{gp0}}{E_s},\ z^* = \frac{z}{d},\ \Delta z^* = \frac{\Delta z}{d} = \frac{L}{dn}$$

where ρ^p, z^* and Δz^* are the normalised GP displacements, normalised depth and normalised elemental length respectively.

Equation (6) is written in finite difference form for elements i = 2 to (n-1) as

$$\left[\frac{\left\{1+\frac{\eta z_i^*}{(L/d)}\right\}}{\Delta z^{*2}} + \frac{\eta}{2\Delta z^*(L/d)}\right]\rho_{i+1}^p - \left[\frac{2\left\{1+\frac{\eta z_i^*}{(L/d)}\right\}}{\Delta z^{*2}}\right]\rho_i^p + \left[\frac{\left\{1+\frac{\eta z_i^*}{(L/d)}\right\}}{\Delta z^{*2}} - \frac{\eta}{2\Delta z^*(L/d)}\right]\rho_{i-1}^p = \frac{4\tau_i}{K_{gp0}E_s} \tag{7}$$

With $a1 = \left[\frac{2\left\{1+\frac{\eta z_i^*}{(L/d)}\right\}}{\Delta z^{*2}}\right]$, $a2 = \frac{\eta}{2\Delta z^*(L/d)}$ and $A = (a1-a2)X\,K_{gp0}/4$,

$B = -a2X\,K_{pg0}/2$, and $C = (a1+a2)X\,K_{pg0}/4$, Eqn. (7) is expressed in the form

$$A\rho_{i-1}^p + B\rho_i^p + C\rho_{i+1}^p = \frac{\tau_i}{E_s} \tag{8}$$

The boundary condition (at $z=0,\ \sigma_z = P/(\pi d^2/4)$) is expressed in terms of axial strain at the top of GP as

$$\varepsilon_{z/z=0} = -\frac{dS^p}{dz} = \frac{P}{(\pi d^2/4)E_{gp0}} \tag{9}$$

The above equation in finite difference form is

$$\frac{S_1^p - S_0^p}{\Delta z} = -\frac{P}{(\pi d^2/4)E_{gp0}} \tag{10}$$

where S_0^p is the mid-point displacement corresponding to an imaginary element at the top. From Eqns. (8) and (10), the displacement equation for the first node may be expressed as

$$\left[A+B\right]\rho_1^p + C\rho_2^p + A\frac{4P\Delta z^*}{\pi E_{gp0}} = \frac{\tau_1}{E_s} \tag{11}$$

Displacement of the element, n, of the GP may be related to the displacements of elements, n-2, n-1 and the base by fitting a third degree of parabola. Using the finite difference scheme with points of non-uniform spacing as per Eqn. (6)

$$\begin{aligned} \frac{dS_n^p}{dz} &= \frac{0.1S_{n-2}^p - 0.67S_{n-1}^p - 0.5S_n^p + 1.067S_{n+1}^p}{\Delta z} \\ \frac{d^2S_n^p}{dz^2} &= \frac{-0.2S_{n-2}^p + 2.0S_{n-1}^p - 5.0S_n^p + 3.2S_{n+1}^p}{\Delta z^2} \end{aligned} \tag{12}$$

Combining Eqns. (6) and (12), the settlement of the nth element is

$$D_{n-2}\rho_{n-2}^p + D_{n-1}\rho_{n-1}^p + D_n\rho_n^p + D_{n+1}\rho_{n+1}^p = \frac{\tau_n}{E_s} \tag{13}$$

where, $D_{n-2} = -0.2(a1-a2)X\,K_{pg0}/4$, $D_{n-1} = (2.0a1-1.34a2)X\,K_{pg0}/4$, $D_n = -(a1-a2)X\,K_{pg0}/4$, $D_{n+1} = (3.2a1-2.12a2)X\,K_{pg0}/4$

To evaluate the settlement of the base of the granular pile i. e., node (n+1), Eqn. (5) is applied as

$$\varepsilon_{z/z=L} = -\frac{dS_{n+1}^p}{dz} = \frac{p_b}{E_{gp0}(1+\eta)} \tag{14}$$

Using again the finite difference scheme for nodes with unequal intervals for the same order of error as in Eqn. (12),

$$\frac{dS_{n+1}^P}{dz} = \frac{S_{n-1}^P - 9.0S_n^P + 8.0S_{n+1}^P}{3.0\Delta z} \tag{15}$$

Thus the settlement of the base is expressed as

$$E_{n-1}\rho_{n-1}^p + E_n\rho_n^p + E_{n+1}\rho_{n+1}^p = \frac{p_b}{E_s} \tag{16}$$

where $E_{n-1} = -n(1+\eta)K_{pg0}d/3L$, $E_n = 3n(1+\eta)K_{pg0}d/L$
$E_{n+1} = -8n(1+\eta)K_{pg0}d/3L$

Combining Eqns. (8), (11), (13) and (16), the GP displacements for nodes i=1 to (n+1) are expressed as

$$\left[I_p\right]\left\{\rho^p\right\} + \left\{X\right\} = \left\{\frac{\tau}{E_s}\right\} \tag{17}$$

where matrices $[I_p]$ and $\{X\}$ are given in the Appendix.

End Bearing Granular Pile : Settlement of the base of a GP resting on a bearing stratum of finite compressibility is approximated by the equation for the displacement of a rigid circular disc on a semi-infinite mass as

$$\rho_b^p = \frac{S_b^p}{d} = \frac{p_b(1-\nu_b^2)\pi/4}{E_b} \tag{18}$$

From the equilibrium equation, the base pressure is expressed in terms of shear stresses

$$p_b = \frac{P}{\pi d^2/4} - \frac{4(L/d)}{n}\sum_{j=1}^{j=n}\tau_j \tag{19}$$

Thus the settlement of the base can be expressed in terms of the applied load and mobilised shear stresses (using Eqns. (18) and (19)) as

$$\rho_b = \left[\frac{P}{E_s \pi d^2/4} - \frac{4(L/d)}{n}\sum_{j=1}^{j=n}\frac{\tau_j}{E_s}\right] \times \frac{\pi(1-\nu_b^2)}{4(E_b/E_s)} \tag{20}$$

Settlement of n^{th} element is estimated as the settlement of the base plus the settlement of the element due to the axial stress acting on it as

$$\rho_n^p = \rho_b^p + \frac{\sigma_n(\Delta z/2d)}{E_{gp}} \tag{21}$$

where σ_n/E_{gp} is axial strain of the n^{th} element and Δz is element length. Thus the settlement of any element i of GP is,

$$\rho_i^p = \rho_b^p + \sum_{j=n}^{j=i-1}\frac{\sigma_j}{E_{gpj}}(\Delta z/d) + \frac{\sigma_i}{E_{gpi}}(\Delta z/2d) \tag{22}$$

The above displacement equations are expressed in matrix form as

$$\left\{\rho^p\right\} = \rho_b\left\{1\right\} + \left[\Delta_1\right]\left\{\frac{\sigma}{E_s}\right\} \tag{23}$$

where $[\Delta_1]$ is upper triangular matrix as per Eqn. (22) incorporating the non-homogeneity of the granular pile. Further using Eqn. (20) for replacing the base displacement, Eqn. (23) can be written as

$$\left\{\rho^{p}\right\}=\frac{P(1-\nu_b^2)}{(E_b/E_s)d^2E_s}\{1\}-\frac{\pi(L/d)(1-\nu_b^2)}{n(E_b/E_s)}[1]\left\{\frac{\tau}{E_s}\right\}+[\Delta_1]\left\{\frac{\sigma}{E_s}\right\} \tag{24}$$

where {1} and [1] are respectively column vector and square matrix of size 'n' in which each term is unity. The shaft shear stresses and axial stresses of elements are related (based on equilibrium relationship) as

$$\sigma_i=\frac{P}{(\pi d^2/4)}-\sum_{j=1}^{j=i-1}\frac{4\tau_j L}{nd}-\frac{2\tau_i L}{nd} \tag{25}$$

The above equation may be written in matrix form for elements i = 1 to n as

$$\left\{\frac{\sigma}{E_s}\right\}=\frac{P}{(\pi d^2/4)E_s}-\frac{4(L/d)}{n}[\Delta_2]\left\{\frac{\tau}{E_s}\right\} \tag{26}$$

where $[\Delta_2]$ is lower triangular matrix of size 'n' in which the diagonal and off diagonal terms are 0.5 and 1.0 respectively.

Using the relationship between axial stresses and shaft shear stresses (Eqn. 26) the final form of displacement equations for elements i = 1 to n in terms of shaft shear stresses (Eqn. (24)) are

$$\left\{\rho^{p}\right\}=\{Y\}+[\Delta]\left\{\frac{\tau}{E_s}\right\} \tag{27}$$

where

$$\begin{aligned}\{Y\}&=\frac{P(1-\upsilon_b^2)}{(E_b/E_s)d^2E_s}\{1\}+\frac{P}{(\pi d^2/4)E_s}[\Delta_1]\{1\}\\ [\Delta]&=-\frac{4(L/d)}{n}[\Delta_1][\Delta_2]-\frac{\pi(L/d)(1-\nu_b^2)}{n(E_b/E_s)}[1]\end{aligned} \tag{28}$$

Compatibility of Displacements

Satisfying the compatibility of displacements of the granular pile and the soil, solutions are obtained in terms of interface shear stresses and displacements. Therefore for floating granular pile, from Eqns. (3a) and (17);

$$\{\rho^{s}\}=\{\rho^{p}\}$$

$$\left\{\frac{\tau}{E_s}\right\}=\left[[1]-[I_p]\right]^{-1}\{X\} \tag{29}$$

For granular pile resting on stiff bearing stratum (Eqns. 3(a) and (27)) the interface shear stresses are

$$\left\{\frac{\tau}{E_s}\right\}=\left[[I_s]-\kappa[I_{sim}]-[\Delta]\right]^{-1}\{Y\} \tag{30}$$

For estimation of κ, an iterative technique suggested by Poulos and Mattes (1969) is used. With an initial chosen value of κ, Eqns. (30) and (19) are solved to estimate the n unknown shear stresses, τ, and base pressure, p_b. Having obtained the solution for chosen value of κ, a closer estimate of the correct value of κ is obtained by considering the compatibility between displacements of soil and the bearing stratum at the pile tip. The soil displacement at the pile tip is

$$\rho_b^s = \frac{S_b^s}{d} = \left\{ I_{bj} - \kappa I_{bjim} \right\} \left\{ \frac{\tau}{E_s} \right\} = \frac{\sum_{j=1}^{j=n} (I_{bj} - \kappa I_{bjim}) \tau_j}{E_s} \tag{31}$$

I_{bj} and I_{bjim} are the displacement influence coefficients for the tip due to shear stresses on real and imaginary elements j respectively. However due to symmetry $I_{bj} = I_{bjim}$. Equating the soil displacement at the pile tip to the displacement of the base due to base stress, p_b (Eqn. 18) the new value of non-dimensional parameter, κ, is obtained as

$$\kappa = 1 - \frac{\pi (1 - \nu_b^2) p_b}{(E_s / E_b) \sum_{j=1}^{j=n} \tau_j I_{bj}} \tag{32}$$

Equation (30) is solved iteratively using the new value of, κ, and the process repeated until the required convergence is obtained for the value of κ. The top settlement of single non-homogeneous granular pile is obtained as

$$S = \frac{P}{E_s d} I \tag{33}$$

where I is settlement influence factor which depends on various parameters related to granular pile and soil. The overall response of the non-homogeneous granular pile is evaluated in terms of settlement influence factor, normalised shear stress distribution along GP-soil interface and percentage of load transferred to the base. Parameters affecting the overall response are (i) length to diameter ratio of the GP, (L/d), (ii) the relative stiffness parameter, $K_{gp0} = (E_{gp0}/E_s)$, (iii) the relative stiffness of the bearing stratum E_b/E_s in case of the end bearing GP (iv) the degree of non-homogeneity of granular pile, η and (v) Poisson's ratio of the soft soil, ν_s and the base ν_b.

Results and Discussion

Results are obtained for the following ranges of non-dimensional parameters;

$K_{gp0} = E_{gp0}/E_s = 10\text{-}400$, $E_b/E_s = 1\text{-}1000$, $\eta = 0\text{-}5$, $\nu_s = 0.5$, $\nu_b = 0.3$, $L/d = 5\text{-}40$.

The results obtained by the above analysis have been validated with those of Mattes and Poulos (1969) and Poulos and Mattes (1969) for single compressible floating and end bearing homogeneous piles (η=0) respectively.

The agreement has been very close as shown in the Table 1.The variation of settlement influence factor, I, with relative GP-soil stiffness parameter, K_{gp0}, for relative length of floating granular pile, L/d=10 and Poisson ratio of surrounding soil, ν_s=0.5, is depicted in Fig. 5. The figure also depicts the effect of degree of non-homogeneity, η. With the increase of relative stiffness parameter, K_{gp0}, the settlement influence factor, I, decreases for all values of non-homogeneity parameter, η. The settlement influence factor decreases with the increase of the degree of non-homogeneity, η. The effect of non-homogeneity is pronounced in the range of K_{gp0} = 10 to 150. The settlement influence factors at K_{gp0} = 50 for η=0, 1, 2 and 4 are 0.225, 0.211, 0.202 and 0.19 respectively. Hence percentage decrease in settlement influence factors in comparison to that of a homogeneous granular pile (η=0) are 6.2, 10.2 and 15.6 for η=1, 2 and 4 respectively. The variation of settlement influence factor with K_{gp0} is shown for a relatively longer floating GP (L/d = 20) in Fig. 6. The trends are similar to those shown in Fig. 5.

The decrease in settlement factor with η for all values of K_{gp0} is less for longer GP in comparison to a shorter GP. The inset in Fig.6 depicts the relative variations of GP moduli for different L/d ratios. For a given degree of non-homogeneity parameter, η, a longer GP would have relatively smaller moduli at all depths compared to a shorter one. A consequence of the above fact is that, the effect of degree of non-homogeneity on I decreases with increasing values of L/d. The settlement influence factors for K_{gp0} = 50 for η = 0, 1, 2 and 4 are 0.209, 0.196, 0.187 and 0.173 respectively. The percentage reductions in settlement influence factors for η = 1, 2 and 4 in comparison to the value for a homogeneous granular pile (η = 0) are thus 6.2, 10.5 and 17.2 respectively for L/d=20.

TABLE 1: Validation of Results with Mattes and Poulos (1969) and Poulos and Mattes (1969)

Parameters		Settlement Influence Factor (I)	Reference
(a)	Floating pile L/d = 10, K_{gp0} = 100, ν_s = 0.5	0.189	Mattes and Poulos (1969)
(b)	End bearing pile L/d = 10, K_{gp0} = 100, ν_s = 0.5, E_b/E_s = 100	0.0776	Poulos and Mattes (1969)
(c)	Floating pile (Same as above)	0.1889	Present Analysis
(d)	End bearing pile (Same as above)	0.07756	Present Analysis

The effect of relative length (L/d) of floating granular pile on settlement influence factor (I) with the degree of non-homogeneity (η) is presented in Fig. 7 for K_{gp0} = 100. As can be expected the settlement influence factor decreases with the increase of η. The rate of decrease of I with η, in case of short granular pile is slightly more due to higher values of modulus of deformation of GP at shallower depths. The settlement influence factors for L/d = 10 and 20 are 0.189 and 0.162 for η = 0 while for η = 2, they are 0.173 and 0.145 respectively. Hence the percentage reductions for L/d = 10 and 20 are 8.5 and 10.5 respectively for η increasing from 0 to 2.

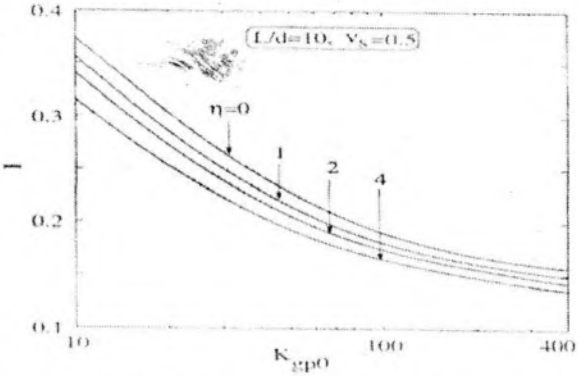

Fig. 5 Variation of I with K_{gp0} for Floating Granular Pile, L/d=10 – Effect of $\bar{\eta}$

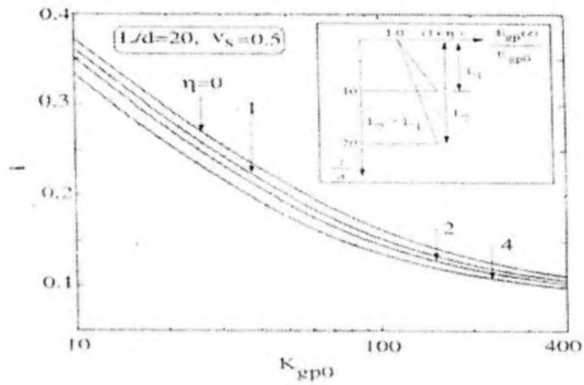

Fig. 6 Variation of I with K_{gp0} for Floating Granular Pile, L/d=20 – Effect of $\bar{\eta}$

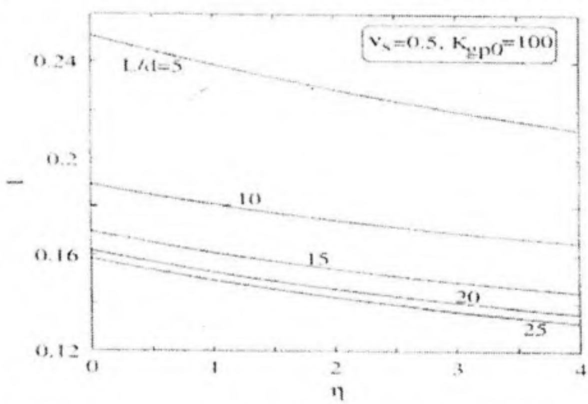

Fig. 7 Variation of I with η for Floating Granular Pile – Effect of L/d

The variation of settlement influence factor with K_{gp0} can be seen in Fig. 8 showing the influence of degree of non-homogeneity (η) for the granular pile (L/d = 10) resting on a stiff bearing stratum (E_b/E_s = 100). The general trends of the curves are similar to those for floating granular pile (Fig. 5). The effect of non-homogeneity of granular pile is pronounced for K_{gp0} in the range 10 to 150.

The settlement influence factors for K_{gp0} = 50 and for η = 0, 1, 2 and 4 are 0.123, 0.102, 0.088 and 0.071 respectively. The percentage decrements in settlement influence factors in comparison to that of homogeneous end bearing granular pile are 17.1, 28.5 and 42.3 for η = 1, 2 and 4 respectively. The effect of non-homogeneity on settlement influence factor decreases with increasing values of K_{gp0}.

Figure 9 shows the variation of settlement influence factor for relatively longer GP (L/d = 20) resting on a stiff bearing stratum (E_b/E_s = 100). The reduction in settlement influence factor with η for smaller values of K_{gp0}, say in the range of 10 to 30, is less. This is due to relatively higher compressibility of granular pile in the upper zone and the presence of bearing strata at depth (as can be seen in the inset). The effect of non-homogeneity is pronounced in the range of K_{gp0} = 30 to 200. The settlement influence factors for K_{gp0} = 100 and for η = 0, 1, 2 and 4 are 0.104, 0.089, 0.079 and 0.066 respectively. The percentage reductions in settlement influence factors with respect to that of a homogeneous granular pile works out to 14.4, 24 and 36.5 respectively. Thus the percentage reduction in settlement decreases with the increase of degree of non-homogeneity, η.

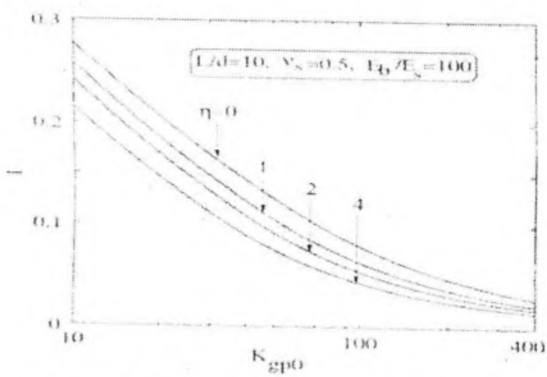

Fig. 8 Variation of I with K_{gp0} for End-bearing Granular Pile, L/d=10 and E_b/E_s=100– Effect of $\bar{\eta}$

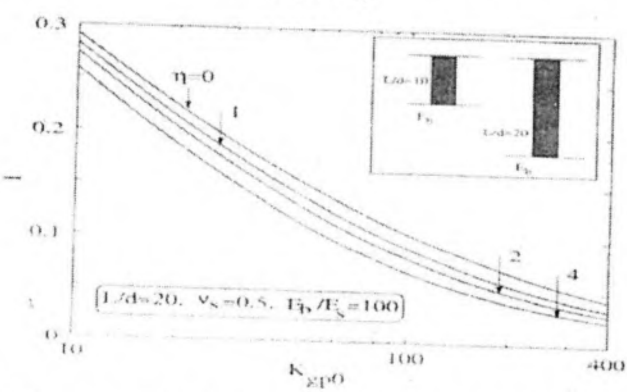

Fig. 9 Variation of I with K_{gp0} for End-bearing Granular Pile, L/d=20 & E_b/E_s=100– Effect of $\bar{\eta}$

Figure 10 shows the variation of settlement influence factor with relative stiffness of the bearing stratum (E_b/E_s) for K_{gp0} = 50 along with the effect of degree of non-homogeneity, η, and relative length of granular pile, L/d. The settlement influence factor decreases as expected with the increase of relative stiffness of bearing stratum due to more load transferred to it. For lower values of E_b/E_s, (3-5), the settlement influence factors of shorter (L/d = 10) GPs are more than those for longer (L/d = 20) GPs. The transition in the relative magnitudes of I with L/d occurs because of the opposite effects of L/d and η. Settlement influence factor, I, decreases with L/d but with η having larger effect in case of shorter GPs. Therefore, end bearing shorter GPs have smaller settlement influence factors for higher values of E_b/E_s. The rate of decrease of settlement influence factor with E_b/E_s is more in case of relatively shorter granular pile (L/d = 10) due to the presence of the bearing stratum at a shallower depth. The percentage reductions in settlement influence factors in case of floating granular pile (E_b/E_s = 1) for L/d = 10 and 20 are both approximately 6.2 for η = 1. For the end bearing granular pile (E_b/E_s =1000) the percentage reductions in settlement with respect to that of a homogeneous granular pile (η = 0), are 18.2 and 9.5 for η = 1 and L/d = 10 and 20 respectively. The percentage reductions in settlement reduction factors for η = 2 for floating (E_b/E_s = 1) and end bearing granular pile (E_b/E_s = 1000) are 10.2 and 29.8 for L/d = 10 while in case of L/d = 20 reductions are 10.5 and 17 respectively. The effect of non-homogeneity on the settlement reduction is thus pronounced in case of short granular pile resting on stiff bearing stratum.

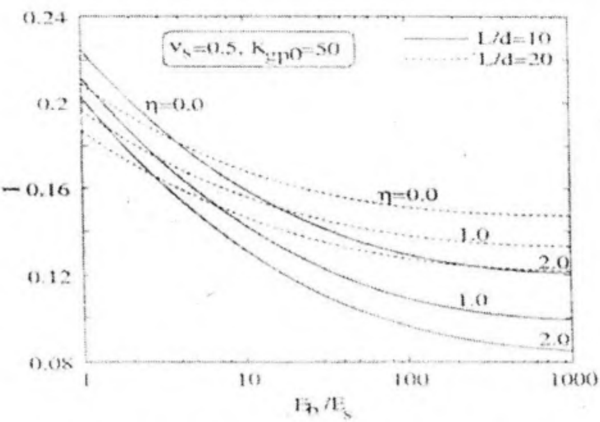

Fig. 10 Variation of I with E_b/E_s – Effect of L/d and η

The effect of relative length of the granular pile (L/d) and relative stiffness of bearing stratum (E_b/E_s) on settlement influence factor (I) with non-homogeneity parameter (η) is presented in Fig. 11 for K_{gp0} = 50. The rate of decrease of settlement influence factor with η is more for relatively shorter granular piles (L/d = 5 & 10). In case of longer granular pile (L/d = 40) the effect of non-homogeneity is less on settlement influence factor due to the presence of the bearing strata at great depth. As had been discussed in previous paragraphs, very less load is transferred to the lower reaches of a long homogeneous (η = 0) compressible GP. The same phenomenon had been reported by Mattes and Poulos (1969) and Scott (1981). Consequently, even if the modulus of deformation of the GP is higher (η > 0) due to non-homogeneity, its consideration to a reduction in settlement would be very little. For the same reason, settlements of long GP (L/d = 40) on a bearing stratum are little affected by the relative stiffness of the bearing stratum. The values of I for L/d = 40, are very close for the case E_b/E_s = 50 and 1000, a twenty fold increase in the bearing stratum stiffness. The effect of relative stiffness of bearing stratum on settlement influence factor is more for shorter GP and its effect increases with increase of non-homogeneity parameter. Settlement influence factors for E_b/E_s = 50 and 1000 are 0.076 and 0.068 respectively for L/d =10 and η = 4.

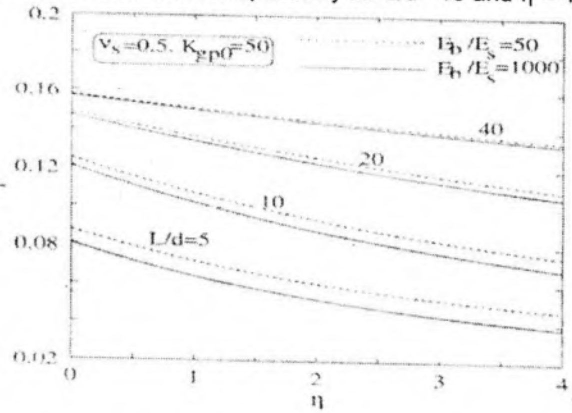

Fig. 11 Variation of I with η – Effect of L/d and E_b/E_s

Variation of normalised shear stress τ^* (= $\tau/(P/\pi dL)$) with normalised depth z^* (= z/L) can be seen in Fig. 12 for L/d =10 and K_{gp0} = 50 showing the effect of non-homogeneity parameter η for a granular pile resting on stiff bearing stratum (E_b/E_s = 100). It is seen that the interface shear stresses in the upper region get reduced due to non-homogeneity of end-bearing granular pile, get transferred to the lower region and the base. Beyond the normalised depth of about z^* = 0.85, shear stresses increase slightly due to transfer of load from the upper region to the lower stiffer region. Shear stresses at these depths are negative and result in a pseudo-down drag effect, i.e., the soil surrounding the GP settles relatively more than the deformation of GP. From the pattern of shear stresses it can be concluded that due to non-homogeneity of granular pile, larger loads are transferred to the base resulting in the reduction of interfacial shear stresses. The effect of non-homogeneity in reducing the interface shear stresses is more for η increasing from 0 to 1 in comparison to η increasing from 1 to 2 or 2 to 4.

Figure 13 shows the variation of normalised shear stresses for relatively longer granular pile (L/d = 20) and K_{gp0} = 100 resting on stiff bearing stratum (E_b/E_s = 1000) showing the effect of the non-homogeneity parameter, η. The trends of the curves are similar to those seen in Fig. 12 except that the slight increase in shear stresses occurs beyond the normalised depth of about z^* = 0.90. It is seen that normalised shear stresses get reduced almost by the same order as in Fig. 12 due to relatively stiffer granular pile and base (K_{gp0} = 100, E_b/E_s = 1000) although the relative length of the granular pile is more. Shear stresses near the region of the bearing stratum are negative (i.e., at normalised depth z^* > 0.90).

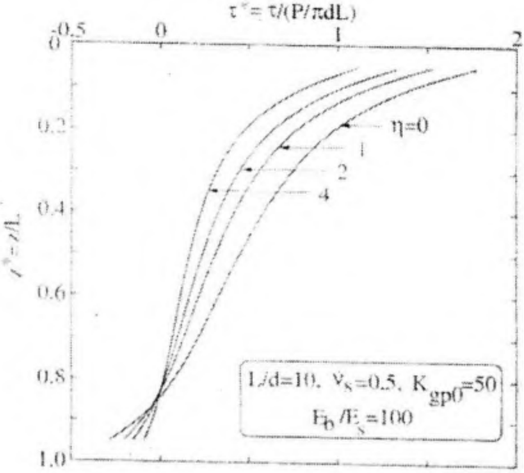

Fig. 12 Variation of τ^* with z^* for End-bearing Granular Pile, L/d=10, K_{gp0}=50 and E_b/E_s=100– Effect of $\bar{\eta}$

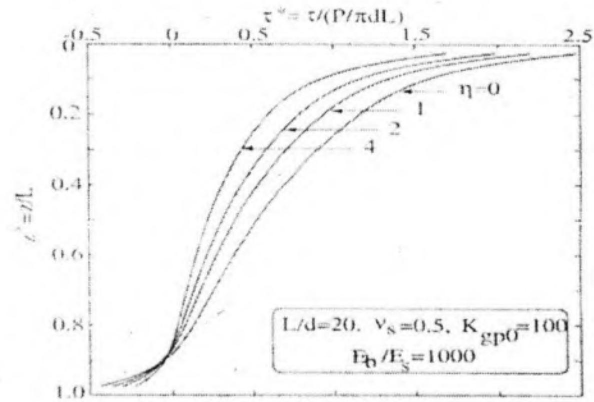

Fig. 13 Variation of τ^* with z^* for End-bearing Granular Pile, L/d=20, K_{gp0}=100 and E_b/E_s=1000– Effect of $\bar{\eta}$

Distribution of normalised axial load, P^* (= P_z/P) with normalised depth z^* (= z/L) of GP resting on stiff bearing stratum (E_b/E_s = 1000) is shown in Fig. 14 for L/d = 20 and K_{gp0} = 100 along with the influence of non-homogeneity parameter, η. As can be expected, the normalised load of GP gets reduced with depth due to transfer of load through interfacial shear stresses. Interestingly, the normalised load in the GP increases slightly for z > 0.9L (approximately) due to negative shear stresses along GP-soil interface (Fig. 13) near the region of rigid bearing stratum. With the increase of degree of non-homogeneity of granular pile, the normalised load along the GP increases at all depths and becomes uniform due to reduction in interfacial shear stresses as seen in Fig. 13. The values of P^* at the base i.e., z^* = 1.0 are 0.35, 0.49, 0.57 and 0.67 for degree of non-homogeneity of GP η = 0, 1, 2 and 4 respectively. The non-homogeneity of granular pile resting on rigid bearing stratum increases the transfer of load to the base significantly. Increment in normalised load on base for η increasing from 0 to 1 is more i.e., 0.14 in comparison to the increase for η increasing 1 to 2 i.e., 0.08 or 2 to 4 i.e., 0.10.

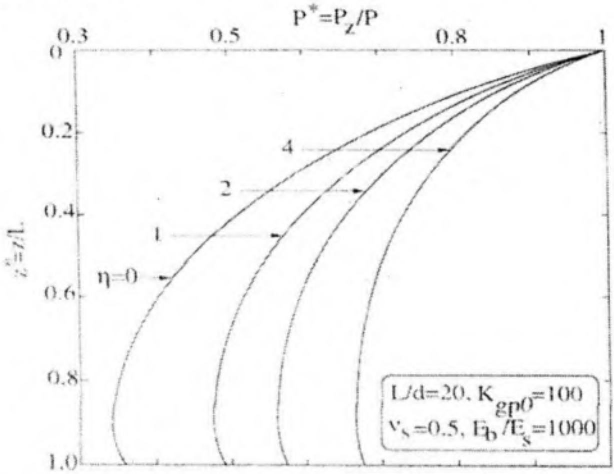

Fig. 14 Variation of P^* with z^* for End-bearing Granular Pile, L/d=20, K_{gp0}=100 and E_b/E_s=1000– Effect of $\bar{\eta}$

The influence of non-homogeneity parameter (η) and the relative stiffness of bearing stratum (E_b/E_s) on distribution of normalised shear stresses with normalised depth is presented in Fig. 15 for L/d = 20 and K_{gp0} = 100. Results are shown for homogeneous (η = 0) and non-homogeneous granular pile (η = 2) for the floating (E_b/E_s = 1), soft (E_b/E_s = 10) and stiff (E_b/E_s = 100) base conditions. Firstly comparing the variation of normalised shear stress variations with depth for a homogeneous (η = 0) and non-homogeneous (η = 2) floating GP, it can be observed that non-homogeneity in deformation modulus causes a reduction in the shear stresses in the top half and an increase of the stresses in the lower half of GP. The shear stresses for η = 2 are more uniform compared to the stresses for η = 0. Interestingly, the depth, above which stresses get reduced and below which they increase, is close to 0.5L. Similar trend in the modification of shear stresses due to the effect of η (> 0), is observed for end bearing (E_b/E_s = 10 and 100) GPs. The neutral point, i. e., the depth above which shear stresses get reduced and below which they increase, moves down with increasing stiffness of the bearing stratum. The depth of the neutral point is close to 0.7L and 0.9L for E_b/E_s = 10 and 100 respectively. For GP resting on a relatively stiff (E_b/E_s = 100) bearing stratum, the shear stresses below the neutral point are negative for both for η = 0 and 2. The load applied to the GP gets transferred to the soil in the top 90 % of the GP length (Fig. 14) and base. Consequently, the soil in the bottom 10 % of the stratum settles more than the adjacent pile elements, thus causing a pseudo-down drag effect.

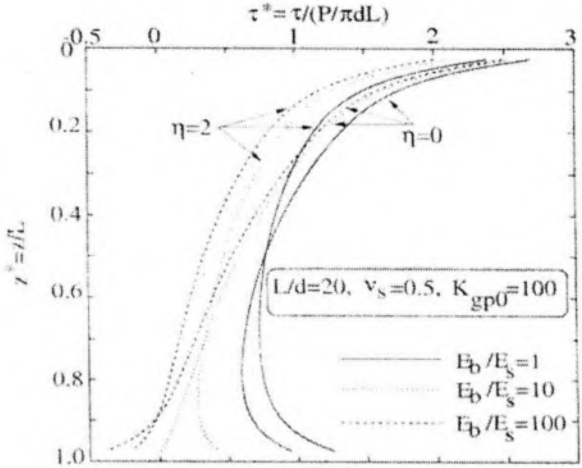

Fig. 15 Variation of τ^* with z^* for End-bearing Granular Pile, L/d=20, K_{gp0}=100– Effect of η and E_b/E_s

The variation of the percentage base load, $(P_b/P)\times100$, with non-homogeneity parameter, η, can be seen in Fig. 16 for $K_{gp0} = 50$ and $E_b/E_s = 100$ for different L/d. The percentage base load increases with the non-homogeneity parameter due to transfer of more load from the top region of granular pile to the base. The base load is larger for short granular pile, due to the presence of stiff bearing stratum at a shallower depth. In case of short granular pile (L/d=5), the rate of increase of the base load with η is less due to higher load transferred to base even for a homogeneous GP ($\eta = 0$). For a long granular pile (L/d=40), this rate is also less due to the presence of bearing stratum at great depth. The percentage base loads for L/d = 10 for $\eta = 0$ and 4 are 50 and 74 respectively while for L/d = 40 the corresponding values are 6 and 20 respectively.

Figure 17 shows the variation of percentage base load, $(P_b/P)\times100$, with relative stiffness of bearing stratum, E_b/E_s, for different non-homogeneity parameter (η) and relative length of granular pile (L/d) for $K_{gp0} = 100$. The base load increases both with relative stiffness of the bearing stratum (E_b/E_s) and the non-homogeneity parameter η. For the floating granular pile ($E_b/E_s = 1$), the effect of non-homogeneity of granular pile on base load is insignificant. The percentage increment in base load for η increasing from 0 to 1 is more in comparison to the increase for η increasing 1 to 2 for any relative length of the pile. In case of long granular pile the percentage base load is less in comparison to the base load for a short granular pile as established in Fig. 16. The effect of non-homogeneity of granular pile on base load increases with the increase in the relative stiffness of the bearing stratum. For $E_b/E_s \geq 1000$ the bearing stratum is almost rigid and the percentage base load becomes nearly constant.

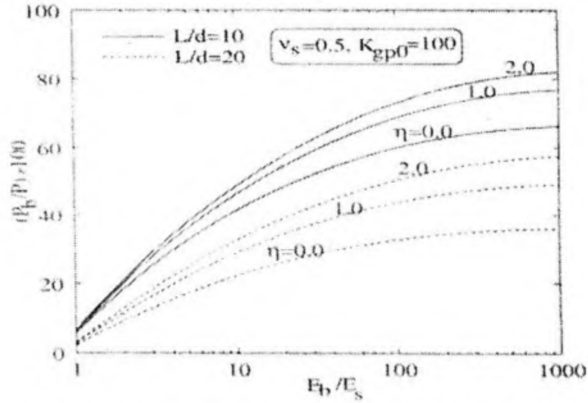

Fig. 16 Variation of Percentage Base Load with η- Effect of L/d

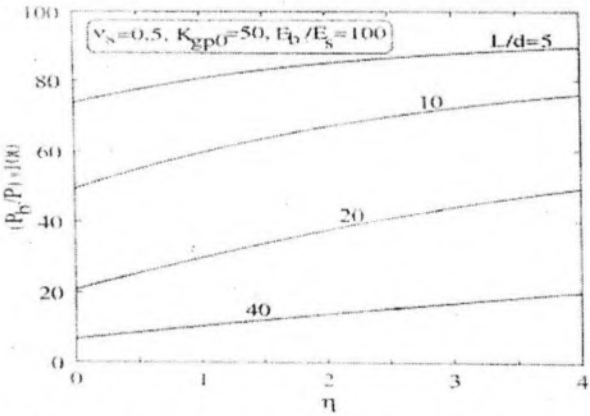

Fig. 17 Variation of Percentage Base Load with E_b/E_s - Effect of L/d and $\tilde{\eta}$

Conclusions

Numerical solutions for the top displacement, normalised shear stresses, load distribution and percentage of load transferred to base are obtained for non-homogeneous floating and end bearing granular piles based on elastic continuum approach described previously by Mattes and Poulos (1969). Formulation for pile elemental displacement equations to incorporate the non-homogeneity parameter for floating and end bearing GPs are presented. Consideration of non-homogeneity of GP in the analysis reflects its true behaviour and accounts for the changes in the state of the GP and in-situ soil due to installation, stiffening and improvement effects. Specific conclusions arrived at from the above analysis are as follows:

1. In the case of a floating non-homogeneous granular pile the reductions in settlement with respect to the homogeneous granular pile are in the range of 10 to 15 % depending on the degree of non-homogeneity.

2. The reduction in settlement for end-bearing non-homogenous granular pile is in the range of 20 to 40 %, depending on the relative stiffness of the bearing stratum and degree of non- homogeneity.

3. Non-homogeneity of granular pile has a marked influence on the variation of shear stresses along GP-soil interface with depth. Depending on the degree of non-homogeneity, the stresses along GP-soil interface get transferred from the top to lower portion of the pile and to the pile-base.

4. Depending on the degree of non-homogeneity of granular pile resting on bearing stratum, the axial load distribution along GP depth gets increased due to reduction in its interfacial shear stresses. The reductions in interfacial shear stresses are mainly due to transfer of major part of load to bearing stratum.

5. Percentage of load transferred to the pile base increases with the increase of degree of non-homogeneity of the GP. In case of end-bearing granular pile this increase is significant depending on the depth of the bearing strata.

Consideration of the non-homogeneity of the granular pile in the analysis represents the in-situ behaviour of granular pile, and the results of the above analysis can be used for the more rational design of granular piles/sand compaction piles.

Acknowledgement

The reviewers' comments are appreciated as they helped in improving the quality of the paper.

Appendix

$[I_p]$ is a square matrix of size, (n+1) of pile displacement influence coefficients and {X}, is a column vector of size, (n+1) and expressed as

$$\{X\} = \begin{Bmatrix} \dfrac{4A(P/E_s d^2)(L/d)}{n\pi K_{gp0}} \\ 0 \\ 0 \\ - \\ 0 \end{Bmatrix} ; [I_p] = \begin{bmatrix} [A+B] & C & 0 & - & - & - & - & 0 & 0 & 0 \\ A & B & C & - & - & - & - & - & - & 0 \\ 0 & A & B & C & - & - & - & - & - & - \\ 0 & 0 & - & - & - & - & - & - & - & - \\ - & - & - & - & - & - & - & - & - & - \\ - & - & - & - & - & - & - & - & - & - \\ - & - & - & - & - & - & - & - & - & - \\ - & - & - & - & - & - & A & B & C & 0 \\ - & - & - & - & - & - & D_{n-2} & D_{n-1} & D_n & D_{n+1} \\ - & - & - & - & - & - & - & E_{n-1} & E_n & E_{n+1} \end{bmatrix}$$

References

Aboshi, H., Ichimoto, E., Enoki, M. and Harda, K. (1979): "The Compozer- A Method to Improve Characteristics of Soft Clays by Inclusion of Large Diameter Sand Columns", *Proc. Int. Conf. on Soil Reinforcement: Reinforced Earth and Other Techniques,* Paris, Vol. 1, pp. 211-216.

Alamgir, M., Miura, N., Poorooshasb, H.B. and Madhav, M.R. (1996): "Deformation Analysis of Soft Ground Reinforced by Columnar Inclusions". *Computers and Geotechnics*, 18(4), pp. 267-299.

Baez, J.I. and Martin G.R. (1992): "Quantitative Evaluation of Stone Column Techniques for Earthquake Liquefaction Mitigation". *X^{th} World Conf. on Earthquake Engineering,* Rotterdam, pp. 1477-1483.

Baez, J.I. and Martin G.R. (1995): "Permeability and Shear Wave Velocity of Vibro-replacement Stone Columns". *Proc. of Geotechnical Engineering. Division of ASCE on Soil Improvement for Earthquake Hazard Mitigation.* Ed. by R.D. Hryciw, Geotechnical Special publication, No. 49, pp. 66-81.

Balaam, N.P. and Booker, J.R. (1981): "Analysis of Rigid Raft Supported by Granular Piles". *Int. Jl. for Numerical and Analytical Methods in Geomechanics,* Vol. 5, pp. 379-403.

Bhandari, R.K.M. and Nayak, N.V. (1984): "Guidelines for Design and Execution of Stone Column Foundation System". *Proc. Indian Geotechnical Conference,* Banglore, Vol. 2, pp. 21-25.

Butterfield, R. and Banerjee, P.K. (1971): "The Elastic Analysis of Compressible Piles and Pile Groups". *Geotechnique*, 21(1), pp. 43-60.

Canneta, G. and Nova, R. (1989): "A Numerical Method for the Analysis of Soft Ground Improved by Columnar Inclusions". *Computers and Geotechnics*, Vol. 7, pp. 99-114.

Datye, K.R. and Nagaraju, S.S. (1975): "Installation and Testing of Rammed Stone Columns". *Proc. Indian Geotechnical Society Speciality Session, 5^{th} Asian Regional Conference on Soil Mechanics and Foundation Engineering,* Banglore, pp. 101-104.

Greenwood, D.A. and Kirsch, K. (1983): "Specialist Ground Improvement by Vibratory and Dynamic Methods-State of the Art Report". *Proc. Int. Conf. on Piling and Ground Treatment for Foundations, Inst. of Civil Engineers,* London, pp. 17-45.

Hu, W., Wood, D.M. and Stewart, W. (1997): "Ground Improvement Using Stone Column Foundations: Results of Model Tests". *Proc. Int. Conf. on Ground Improvement Techniques,* Macau, pp. 247-256.

Mattes, N.S. and Poulos, H.G. (1969): "Settlement of Single Compressible Pile". *Jl. of Soil Mechanics and Foundations Division, ASCE*, 95(SM1), pp. 189-207.

Mitchell, J.K. and Solymer, Z.V. (1984): "Time Dependent Strength Gain in Freshly Deposited or Densified Sand". *Jl. of Geotechnical Engineering Division, ASCE*, 110(11), pp. 1559-1575.

Mizuno, Y., Suematsu, N. and Okuyama, K. (1987): "Design Methods of Sand Compaction Pile for Sandy Soils Containing Fines". *Tsuchi-to-Kiso, Japanese Society of Soil Mechanics and Foundation Engineering*, 35(5), pp. 21-16.

Nakayama, J., Eizabuno, I., Hideo, K. and Soichi, T. (1973): "On Stabilisation Characteristics of Sand Compaction Piles". *Japanese Society of Soil Mechanics and Foundation Engineering*, 13(3), pp. 61-68.

Nayak, N.V. (1983): "Recent Advances in Ground Improvement by Stone Column". *Proc. Indian Geotechnical Conference,* Madras, Theme No. V, pp. 19-24.

Poorooshasb, H.B. and Meyerhoff, G.G. (1997): "Analysis of Behaviour of Stone Columns and Lime Columns". *Computers and Geotechnics*, 20(1), pp. 47-70.

Poulos, H.G. and Mattes, N.S. (1969): "The Behaviour of Axially Loaded End-bearing Piles". *Geotechnique*, Vol. 19, pp. 285-300.

Schweiger and Pandey, G.N. (1986): "Numerical Analysis of Stone Column Supported Foundations". *Computers and Geotechnics*, Vol. 2, pp. 347-372.

Scott, R.F. (1981): *Foundation Analysis*, Prentice-Hall. Inc., Englewood Cliffs, NJ, pp. 545.

Seed, H.B. and Booker, J.R. (1977): "Stabilization of Potentially Liquefiable Deposits Using Gravel Drains". *Jl. of Geotechnical Engineering Division, ASCE*, 103(7), pp. 757-768.

Shamoto, Y., Katsura, Y., Katsuyuki, T. and Zhang, J.M. (1997): "A Simplified Method for Evaluating the Effectiveness of Compaction Piles in Sands Containing Fines". *Japanese Society of Soil Mechanics and Foundation Engineering*, 37(1), pp. 89-96.

Solymer, Z.V., Osellame, J. and Basuki, J.P. (1986): "Ground Improvement by Compaction Piling". *Jl. of Geotechnical Engineering Division, ASCE*, 112(12), pp. 1069-1083.

Van Impe, W.F. and Madhav, M.R. (1992): "Analysis and Settlement of Dilating Stone Column Reinforced Soil". *Osterreichische Ing. und Arch.-Zeitschrift*, Vol. 137, pp. 114-121.